# Spatial separation of collinearly emitted broadband frequency-correlated photon pairs

Yuki Kamei [ORCID],[*] Cao Bo [ORCID],[*] Ryo Okamoto [ORCID],[*] and Shigeki Takeuchi [ORCID][†]

*Department of Electronic Science and Engineering, Kyoto University, Kyotodaigakukatsura, Nishikyo-ku, Kyoto 615-8510, Japan*

We experimentally study the separation of broadband photon pairs that share the same properties in all degrees of freedom. We find that broadband photon pairs with a bandwidth of about 90 nm can be efficiently separated using time-reversed Hong-Ou-Mandel (HOM) interference. The frequency correlation of the separated photons is verified through joint spectral intensity measurements. The visibility of the HOM interference between the separated photons is shown to be higher than the classical limit of 50%, ensuring that the separated photons are indistinguishable. These results may contribute to improving the performance of quantum sensing and quantum communication.

Quantum technologies using photons have advanced considerably over the past two decades, including quantum communication [1,2], quantum computation [3–5], and quantum sensing [6–13]. For these applications, entangled photons are considered an important resource for realizing the advantages of quantum phenomena. In particular, frequency-entangled photons have attracted attention for their wide range of potential applications, such as quantum optical coherence tomography [14–18], dense quantum key distribution [19], and nonlinear absorption spectroscopy [20,21]. Bulk nonlinear crystals have been widely used for generating frequency-entangled photons. However, the low conversion efficiency of such bulk nonlinear crystals may prevent the practical application of entangled photon pairs. To overcome this problem, entangled photon generation in waveguide structures has been developed and has received growing attention [22–24]. Recently, efficient generation of broadband frequency-entangled photons has been realized using a chirped quasi-phase-matching device with a waveguide structure [25]. However, when using such a waveguide photon-pair source, photon pairs are generated in the same spatial and polarization mode and these photons cannot be directly used for applications requiring spatially separated indistinguishable photons, such as quantum optical coherence tomography [14–18], quantum phase measurement [6–8], and quantum super-resolution [26–28]. Note that the type-II phase-matching condition enables us to efficiently separate the photons in a pair generated in a waveguide device, but the conversion efficiency is one order of magnitude lower than that for the type-0 phase-matching condition [29,30].

In a pioneering study, Burlakov *et al.* used time-reversed Hong-Ou-Mandel (HOM) interference to separate collinearly emitted two photons that share the same properties in all degrees of freedom: spatial, frequency, and polarization [31]. The same method has been used to separate photons generated

in an optical fiber [32] and a silicon waveguide [33]. However, in these experiments, the bandwidth of the separated two photons has been limited to 40 nm [31], and frequency correlation of the separated photons has not been directly observed. The broad bandwidth of separated photons entangled in frequency is crucially important for some applications, such as quantum optical coherence tomography [14–18] and dense quantum key distribution [19].

In this Letter, we experimentally demonstrate the separation of broadband photon pairs that share the same properties in all degrees of freedom. We show that broadband photon pairs with bandwidths of about 90 nm can be efficiently separated using time-reversed HOM interference. The frequency correlation of the separated photons is verified through joint spectral intensity measurements. The visibility of the HOM interference between the separated photons is shown to be higher than the classical limit of 50%, ensuring the indistinguishability of them.

First we theoretically explain how a collinearly emitted photon pair can be spatially separated through time-reversed HOM interference while preserving the frequency correlation. As shown in Fig. 1, we assume that there are two identical nonlinear crystals. Each crystal is pumped by a laser beam divided by a beam splitter and generates two photons correlated in frequency, which share the same spatial and polarization mode. When the average number of photon pairs generated per mode in each source is much lower than 1, the quantum state after the crystals can be given as follows:

$$\int (\Psi(\omega)|\Omega + \omega, \Omega - \omega\rangle_a |0\rangle_b - e^{i2\phi}\Psi(\omega)|0\rangle_a |\Omega$$
$$+ \omega, \Omega - \omega\rangle_b)/\sqrt{2}\, d\omega, \tag{1}$$

where $\phi$ is the phase difference between the input modes $a$ and $b$, and $\Psi(\omega)$ is the normalized spectral probability amplitude for the photon pair. We assume that the input photons are anticorrelated in frequency $\omega$ around the center frequency $\Omega$. This state is entangled in the photon number, the so-called "NOON" state. After quantum interference at the 50:50 beam

---
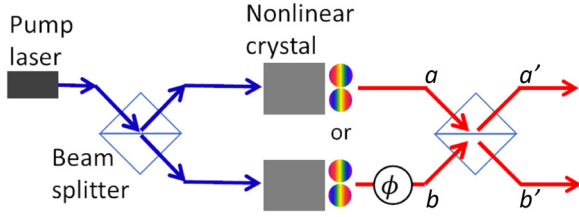
FIG. 1. Schematic of time-reversed HOM interference. $a$ and $b$ are the input modes of the beam splitter, $a'$ and $b'$ are the output modes of the beam splitter, and $\phi$ is the phase difference between the input modes.

splitter, the output state can be written as

$$\frac{(1+e^{i2\phi})}{2}\int \Psi(\omega)|\Omega+\omega\rangle_{a'}|\Omega-\omega\rangle_{b'}d\omega$$

$$+\frac{(1-e^{i2\phi})}{2\sqrt{2}}\int \Psi(\omega)(|\Omega+\omega,\Omega-\omega\rangle_{a'}|0\rangle_{b'}$$

$$-|0\rangle_{a'}|\Omega+\omega,\Omega-\omega\rangle_{b'})d\omega. \tag{2}$$

Thus, when phase $\phi$ is 0, the two photons are completely separated at the output as

$$\int \Psi(\omega)|\Omega+\omega\rangle_{a'}|\Omega-\omega\rangle_{b'}d\omega, \tag{3}$$

which is perfectly entangled in frequency.

Figure 2 shows the experimental setup. A pump laser beam with a wavelength of 405 nm is divided into two paths by a broadband nonpolarizing BS. The simultaneous pumping of a 2-mm-long BBO crystal from both surfaces yields a two-photon NOON state with a center wavelength of 810 nm entangled in the clockwise and counterclockwise paths. Then, the entangled state is injected into the BS and is transformed through two-photon quantum interference. The quantum state for the output photon changes depending on the phase $\phi$ in the interferometer as shown in Eq. (2). $\phi$ is controlled by a Berek polarization compensator (5540M, Newport), which creates a phase difference between the pump and the generated photons. The Fig. 2 inset shows the spectrum of the generated photons measured with a commercial spectrometer (Acton SP2300, Princeton Instruments). The full width at half maximum (FWHM) of the spectrum is about 90 nm. The separated photons (signal photons and idler photons) are evaluated by three different setups: (I), (II), and (III) in Fig. 2.

To check how many photon pairs are spatially separated, we used a coincidence measurement system [dashed square (I) in Fig. 2]. If the photons are successfully separated, each photon is coupled into a single-mode fiber (P1-780PM-FC-2, Thorlabs) and guided to a single-photon detector (SPCM-AQRH-14-FC, Excelitas Technologies), contributing to the coincidence event. Figure 3(a) shows the coincidence counts while changing phase $\phi$, using bandpass filters (BPFs in Fig. 2) with a bandwidth of 4 nm. Note that phase $\phi$ given by the Berek polarization compensator for each setting was calculated from the Sellmeier equation of $MgF_2$. The coincidence count at the output varies depending on $\phi$ as predicted by Eq. (2). At $\phi$ where the coincidence count reaches the
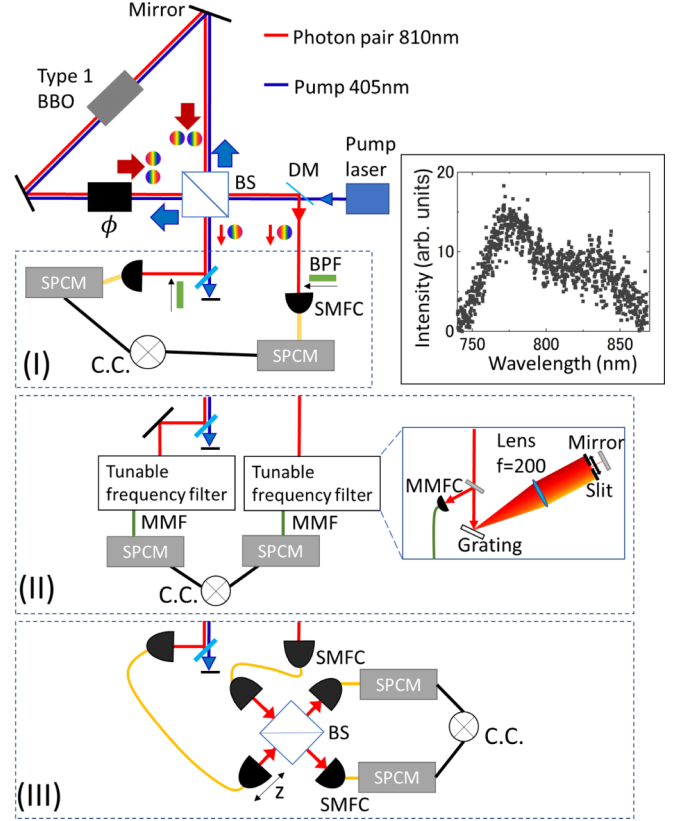


FIG. 2. Schematic of experimental setup for efficient separation of broadband photons. The inset shows the measured generated photon spectrum. The separated photons are evaluated by three different measurement setups: coincidence measurement (I), frequency correlation measurement (II), and two-photon quantum interference (III). The inset shows the spectrum of the generated photons measured with a spectrometer. Abbreviations: DM: dichroic mirror; BS: beam splitter; BBO: $\beta$-barium borate; BPF: band pass filter; SPCM: single-photon counting module; SMFC: single-mode fiber coupler; MMF: multimode fiber; MMFC: multimode fiber coupler; C.C.: coincidence counter.

maximum value, the photons are maximally separated. The visibility of the observed fringe is $79 \pm 1\%$. To directly investigate the photon-pair separation performance, we evaluate the percentage of separated photon pairs relative to the total number photon pairs, which is defined as $R = N_{max}/(N_{max} + N_{min})$, where $N_{max}$ and $N_{min}$ are the maximum and minimum coincidence counts of the fringe, respectively. Since visibility $V$ is defined as $V = (N_{max} - N_{min})/(N_{max} + N_{min})$, $R$ can be represented with $V$ as $R = (1 + V)/2$. Thus, when we used the bandpass filter, $R$ is given by $(1 + 0.79)/2 = 0.90$, showing that 90% of the input photon pairs are separated at the output. Figure 3(b) shows the phase dependence of the coincidence counts without the bandpass filters. In this case, the photon pairs have a bandwidth of 90 nm as shown in the inset of Fig. 2. The observed fringe has a visibility of $40 \pm 2\%$ and, thus, $R$ is given by $(1 + 0.40)/2 = 0.70$, showing that 70% of the input photon pairs are separated at the output. The degradation of the visibility of the broadband photons can be explained by the spatial mode mismatch at the BS, the

(a)



(b)
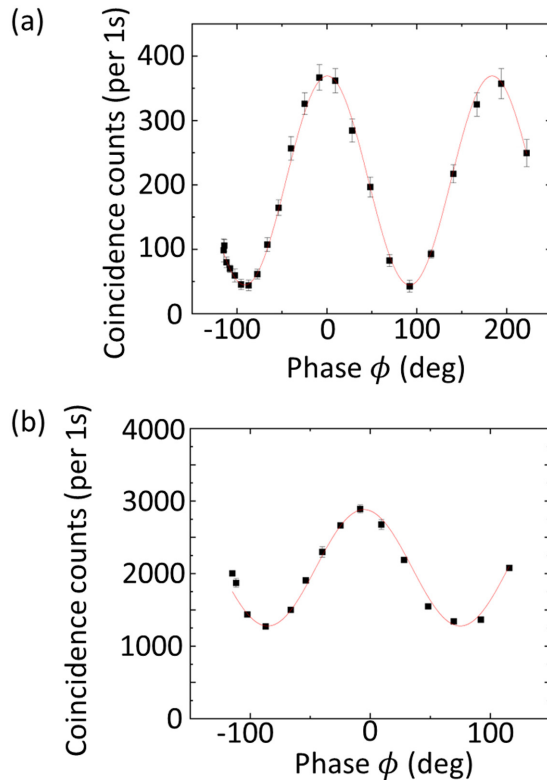


FIG. 3. Coincidence counts while changing phase $\phi$ measured (a) with bandpass filters and (b) without bandpass filters. The black dots are the experimental data, and the red curves are the sinusoidal fitting curves. The error bars are the standard deviation of ten independent measurements.



FIG. 4. Frequency-resolved coincidence detection of separated photon pairs. The horizontal and vertical axes are the wavelengths of the signal and idler photons, respectively.

chromatic dispersion and the losses asymmetrically suffered by the clockwise and counterclockwise photon pairs.

Next, we checked the frequency correlation of the spatially separated photon pairs. For this, we used measurement system (II) in Fig. 2. Each photon is guided to a tunable frequency filter, consisting mainly of a grating and a slit. By selecting the slit position, we can tune the wavelength of a photon with a resolution of 5 nm. After passing through the tunable frequency filter, the photons are detected by single-photon detectors. The two-photon joint spectrum was obtained by recording the coincidence counts while scanning the wavelength settings of both tunable frequency filters. As shown in Fig. 4, the observed joint spectrum is diagonally distributed, indicating that the separated photons have a frequency correlation. The coincidences that are not exactly on the diagonal line can be explained by the resolution of the variable frequency filter (5 nm). Because the accidental coincidence counts are too small to be detected, the counts for the off-diagonal component are zero. The wavelength range for the diagonal component in which the coincidence counts are larger than 0 spans 100 nm. The coincidence distribution is asymmetric as can be seen from Fig. 4: the peak of the coincidence counts is at the intersection of the signal wavelength of 780 nm and the idler wavelength of 840 nm. This asymmetry can be explained by the difference in the transmission spectra of the tunable frequency filters: the tunable frequency

filter used for idler photons has a higher transmittance at longer wavelengths. Note that the effect of the dispersion of the Berek polarization compensator to the joint spectrum is negligibly small.

Finally, we performed two-photon interference between separated photons with setup (III) in Fig. 2. The separated photon pairs were guided to a BS to check the quality of the two-photon quantum interference. Figure 5 shows the coincidence counts while changing the relative delay between the photons. A clear dip is observed, and we obtain a visibility of $58 \pm 5\%$, which is higher than the classical limit of 50% [34,35]. The FWHM for the dip is $2.3 \pm 0.2$ μm, which agrees
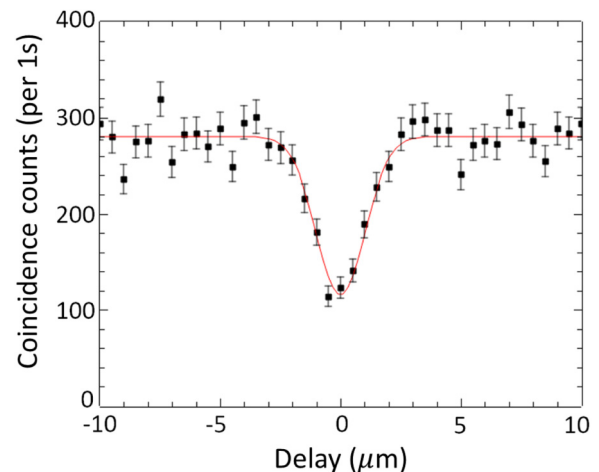


FIG. 5. Two-photon interference for separated photon pairs. The black dots are the experimental data, and the red curve is the Gaussian fitting curve. The error bars are calculated assuming Poisson count statistics. Since the error bars correspond to one $\sigma$ or 68% confidence intervals, we do not expect the fitting curve to lie within the error bars of the data points more than 68%. On the other hand, the large deviation of some data points from the fitting curve may be due to extra noise, such as the fluctuation of pump laser power.

well with the theoretical value (2.28 μm) calculated from the bandwidth of the observed spectrum (inset in Fig. 2).

In conclusion, we have experimentally demonstrated the separation of broadband photon pairs that share the same properties in all degrees of freedom. In our experiment, 70% of input broadband photons with a bandwidth of 90 nm were successfully separated using time-reversed HOM interference. We verified the frequency correlation of the separated photons through joint spectral intensity measurements. Then, we performed HOM interference measurements between the separated photons and found that the observed visibility of 58% clearly exceeds the classical limit of 50%, ensuring the indistinguishability of the separated photons.

[1] N. Gisin and R. Thew, Nat. Photonics **1**, 165 (2007).

[2] H. J. Kimble, Nature (London) **453**, 1023 (2008).

[3] J. L. O'Brien, Science **318**, 1567 (2007).

[4] R. Okamoto, J. L. O'Brien, H. F. Hofmann, T. Nagata, K. Sasaki, and S. Takeuchi, Science **323**, 483 (2009).

[5] T. Ono, R. Okamoto, M. Tanida, H. F. Hofmann, and S. Takeuchi, Sci. Rep. **7**, 45353 (2017).

[6] V. Giovannetti, S. Lloyd, and L. Maccone, Nat. Photonics **5**, 222 (2011).

[7] T. Nagata, R. Okamoto, J. L. O'Brien, K. Sasaki, and S. Takeuchi, Science **316**, 726 (2007).

[8] R. Okamoto, H. F. Hofmann, T. Nagata, J. L. O'Brien, K. Sasaki, and S. Takeuchi, New J. Phys. **10**, 073033 (2008).

[9] R. Okamoto, M. Iefuji, S. Oyama, K. Yamagata, H. Imai, A. Fujiwara, and S. Takeuchi, Phys. Rev. Lett. **109**, 130404 (2012).

[10] T. Ono, R. Okamoto, and S. Takeuchi, Nat. Commun. **4**, 2426 (2013).

[11] R. Okamoto, S. Oyama, K. Yamagata, A. Fujiwara, and S. Takeuchi, Phys. Rev. A **96**, 022124 (2017).

[12] S. Nohara, R. Okamoto, A. Fujiwara, and S. Takeuchi, Phys. Rev. A **102**, 030401(R) (2020).

[13] R. Okamoto, Y. Tokami, and S. Takeuchi, New J. Phys. **22**, 103016 (2020).

[14] A. F. Abouraddy, M. B. Nasr, B. E. A. Saleh, A. V. Sergienko, and M. C. Teich, Phys. Rev. A **65**, 053817 (2002).

[15] M. B. Nasr, B. E. A. Saleh, A. V. Sergienko, and M. C. Teich, Phys. Rev. Lett. **91**, 083601 (2003).

[16] M. Okano, R. Okamoto, A. Tanaka, S. Ishida, N. Nishizawa, and S. Takeuchi, Phys. Rev. A **88**, 043845 (2013).

[17] M. Okano, H. H. Lim, R. Okamoto, N. Nishizawa, S. Kurimura, and S. Takeuchi, Sci. Rep. **5**, 18042 (2016).

[18] K. Hayama, B. Cao, R. Okamoto, S. Suezawa, M. Okano, and S. Takeuchi, Opt. Lett. **47**, 4949 (2022).

[19] S. Wengerowsky, S. K. Joshi, F. Steinlechner, H. Hübel, and R. Ursin, Nature (London) **564**, 225 (2018).

[20] D. A. Kalashnikov, A. V. Paterova, S. P. Kulik, and L. A. Krivitsky, Nat. Photonics **10**, 98 (2016).

[21] Y. Mukai, M. Arahata, T. Tashima, R. Okamoto, and S. Takeuchi, Phys. Rev. Appl. **15**, 034019 (2021).

[22] T. Suhara, Laser Photonics Rev. **3**, 370 (2009).

[23] S. Atzeni, A. S. Rab, G. Corrielli, E. Polino, M. Valeri, P. Mataloni, N. Spagnolo, A. Crespi, F. Sciarrino, and R. Osellame, Optica **5**, 311 (2018).

[24] Z. Yin, K. Sugiura, H. Takashima, R. Okamoto, F. Qiu, S. Yokoyama, and S. Takeuchi, Opt. Express **29**, 4821 (2021).

[25] B. Cao, M. Hisamitsu, K. Tokuda, S. Kurimura, R. Okamoto, and S. Takeuchi, Opt. Express **29**, 21615 (2021).

[26] A. N. Boto, P. Kok, D. S. Abrams, S. L. Braunstein, C. P. Williams, and J. P. Dowling, Phys. Rev. Lett. **85**, 2733 (2000).

[27] Y. Kawabe, H. Fujiwara, R. Okamoto, K. Sasaki, and S. Takeuchi, Opt. Express **15**, 14244 (2007).

[28] L. A. Rozema, J. D. Bateman, D. H. Mahler, R. Okamoto, A. Feizpour, A. Hayat, and A. M. Steinberg, Phys. Rev. Lett. **112**, 223602 (2014).

[29] H. Vanherzeele and J. D. Bierlein, Opt. Lett. **17**, 982 (1992).

[30] H. J. Lee, H. Kim, M. Cha, and H. S. Moon, Appl. Phys. B: Lasers Opt. **108**, 585 (2012).

[31] A. V. Burlakov, M. V. Chekhova, O. A. Karabutova, and S. P. Kulik, Phys. Rev. A **64**, 041803(R) (2001).

[32] J. Chen, K. F. Lee, and P. Kumar, Phys. Rev. A **76**, 031804(R) (2007).

[33] J. W. Silverstone, D. Bonneau, K. Ohira, N. Suzuki, H. Yoshida, N. Iizuka, M. Ezaki, C. M. Natarajan, M. G. Tanner, R. H. Hadfield *et al.*, Nat. Photonics **8**, 104 (2014).

[34] L. Mandel, Phys. Rev. A **28**, 929 (1983).

[35] Z. Y. Ou, E. C. Gage, B. E. Magill, and L. Mandel, J. Opt. Soc. Am. B **6**, 100 (1989).